Auroral Signatures of Ballooning Mode Near Substorm Onset: Open Geospace General Circulation Model Simulations

J. Raeder,[1] P. Zhu,[2] Y. Ge,[1] and G. Siscoe[3]

We present results from Open Geospace General Circulation Model simulations of the 23 March 2007 THEMIS "first light" substorm. We investigate the relation between ballooning modes in the tail and auroral "beads." Magnetic mapping of the ballooning structures in the tail shows an ionosphere signature that closely resembles auroral beads. The close match of the ballooning properties in the tail with observations, in particular an azimuthal wavelength of ~0.5 R_E, and the close resemblance of the mapped ballooning structures in the simulation with observed auroral beads provides evidence that beads are a signature of tail ballooning modes. Since the aurora is much easier observed globally than the tail, this result allows studying the relation of ballooning to the substorm phases using auroral observations. From the simulation, we find no direct connection between the ballooning mode and expansion phase onset. However, other instabilities that lie somewhere between ballooning and tearing may play an important role as trigger.

1. INTRODUCTION

Recent global Open Geospace General Circulation Model (OpenGGCM) simulations of substorms show that near expansion phase onset, the tail becomes ballooning mode unstable [*Raeder et al.*, 2010]. Although the ballooning mode has long been implicated as a possible trigger for substorm onset [*Lee and Wolf*, 1992; *Ohtani and Tamao*, 1993; *Vetoulis and Chen*, 1994; *Lee and Min*, 1996; *Pu et al.*, 1997, 1999; *Miura*, 2001; *Bhattacharjee et al.*, 1998; *Cheng and Zaharia*, 2004; *Zhu et al.*, 2007, 2004], it has been difficult to tie theoretical predictions to observations. The key prediction for the ballooning mode in the geomagnetic tail is a non-propagating wave structure in the azimuthal direction of fairly high wavenumber corresponding to a wavelength of ~0.5 R_E. Because the wave does not propagate, and because the orbital motion of satellites in the region of interest is rather slow, there is, under most circumstances, no unique signature to observe. *Saito et al.* [2008] presented Geotail observations that showed convected structures in the region of $X_{\mathrm{GSE}} = -10$ to -13 R_E just before substorm onset that were consistent with ballooning mode structures. Although such observations are encouraging, they do not yet constitute proof that a ballooning mode is present.

If ballooning modes develop in the tail, they might have a visible counterpart in the ionosphere. If the azimuthal wavelength of the ballooning waves were 0.5 R_E, their distance was 10 R_E from the Earth, and if they mapped radially to the ionosphere, their azimuthal wavenumber would be $m = 2\pi 10/0.5 = 130$, and in terms of wavelength, their characteristic size at 70° magnetic latitude would be $l = \cos(70°) \times 0.5/10 = 109$ km. Such auroral structures are indeed reported, for example, by *Henderson* [2009], who shows IMAGE WIC data with auroral "beads" that have just these characteristics. Ground-based auroral "bead" observations were reported by *Liang et al.* [2008] in conjunction with substorm expansion

[1]Space Science Center and Physics Department, University of New Hampshire, Durham, New Hampshire, USA.

[2]Department of Engineering Physics and Department of Physics, University of Wisconsin-Madison, Madison, Wisconsin, USA.

[3]Center for Space Physics, Boston University, Boston, Massachusetts, USA.

Auroral Phenomenology and Magnetospheric Processes: Earth and Other Planets
Geophysical Monograph Series 197

10.1029/2011GM001200

phase onset. In subsequent work, *Liang et al.* [2009] presented a conjunction between ground-based observations of bead-like auroral structures and waves observed by Time History of Events and Macroscale Interactions during Substorms (THEMIS) in the near-Earth tail. The THEMIS waves are interpreted as the Doppler-shifted signature of ballooning modes and the corresponding auroral beads as their auroral counterpart. These observations are probably the most indicative, so far, of a link between ballooning in the tail and wavelike auroral structures. One should keep in mind, however, that such wavelike structures could have other causes such as Kelvin-Helmholtz waves. Also, the waves observed at THEMIS have frequencies in the Pi2 range. Such waves are ubiquitous at substorm onset but generally not associated with the ballooning mode [*Kepko et al.*, 2001, 2008].

Here we present OpenGGCM simulations of the 23 March 2007 THEMIS "first light" substorm [*Raeder et al.*, 2008], which show clear ballooning mode signatures near substorm onset [*Raeder et al.*, 2010]. In the latter paper, we showed that the tail signatures in the simulation are consistent with the predicted and the observed signatures, in particular, the 0.5 R_E wavelength. We now show how these signatures map to the ionosphere. In the following, we briefly describe the model, present the tail signatures, and show how they map to the ionosphere.

2. OPENGGCM MODEL

The OpenGGCM is a global coupled model of the Earth's magnetosphere, ionosphere, and thermosphere. The magnetosphere part solves the MHD equations as an initial-boundary-value problem. The MHD equations are solved to within ~3 R_E of the Earth. The region within 3 R_E is treated as a magnetosphere-ionosphere (M-I) coupling region where physical processes that couple the magnetosphere to the ionosphere-thermosphere system are parameterized using simple models and relationships. The ionosphere-thermosphere system is modeled using the NOAA Coupled Thermosphere Ionosphere Model (CTIM) [*Fuller-Rowell et al.*, 1996; *Raeder et al.*, 2001a]. The OpenGGCM has been described with some detail [see, e.g., *Raeder et al.*, 2001b; *Raeder*, 2003; *Raeder et al.*, 2008]; we thus refer the reader to these papers. In particular, *Raeder et al.* [2008] also discusses a simulation of the same substorm that is further analyzed here.

3. 23 MARCH 2007 SUBSTORM

We chose the 23 March 2007 substorm for this study because it has already been investigated by several groups [*Angelopoulos et al.*, 2008; *Runov et al.*, 2008; *Raeder et al.*, 2008; *Zhu et al.*, 2009] and because we had an OpenGGCM simulation of this substorm available [*Raeder et al.*, 2008]. In the latter paper, we showed that the simulation reproduces the salient features of a substorm that can be expected from a fluid simulation, in particular, the auroral brightening, the development of the westward traveling surge, fast flows in the tail, and the dipolarization of the magnetic field in the near-Earth tail. Of course, there are kinetic features that cannot be modeled with a fluid code, such as particle injections and auroral kilometric radiation. However, with a recently developed new model, in which the OpenGGCM is coupled with Rice Convection Model, we were also able to produce electron and proton injections for the same event, which compared quite well with observations [*Hu et al.*, 2010]. In this paper, we do therefore not address the validity of the simulation but rather investigate in detail the processes that occur just around the time of the onset of the expansion phase in the simulation.

4. TAIL DYNAMICS

The plasma and field dynamics in the tail for this substorm simulation has been shown in the paper by *Raeder et al.* [2010]. Specifically, Figures 4 and 5 in that paper show the development of the finger-like structures that are characteristic of the ballooning mode. The results presented here are from the model run with the higher resolution shown in Figure 5 of *Raeder et al.* [2010]. There, the structures were made visible by projecting quantities such as a velocity component or the imbalance between the magnetic and pressure forces in the cross-tail direction ($\tilde{F}_y = (\mathbf{j} \times \mathbf{B} - \nabla p)_y$) onto the tail current sheet. Such a projection is necessary because this is a simulation of a real event with measured solar wind and interplanetary magnetic field data as input to the simulation and with a realistic dipole tilt. Thus, the center of the current sheet is not a plane, but a surface that is tilted and undulating. However, it is still well defined by the condition $B_x = 0$. The quantity $\tilde{F}_y$ is particularly useful because it shows the ballooning mode most clearly. Figure 1 shows a different projection of the ballooning fingers, in this case, a spatial cut at $X_{\mathrm{GSE}} = -16\ R_E$. The cuts are taken at times 10:30, 10:32, 10:34, and 10:36 UT, respectively. The figure shows clearly how the fingers develop. They start out in the center of the plasma sheet, and then spread in both azimuthal directions, but predominantly toward dawn. The spreading of the instability occurs through addition of new fingers, while their spacing, i.e., the wavelength of the mode, remains largely unchanged. Figure 5 of *Raeder et al.* [2010] also shows that at later times, the entire structure moves dawnward (compare second to third row); however, in this paper, we will only consider the early development.

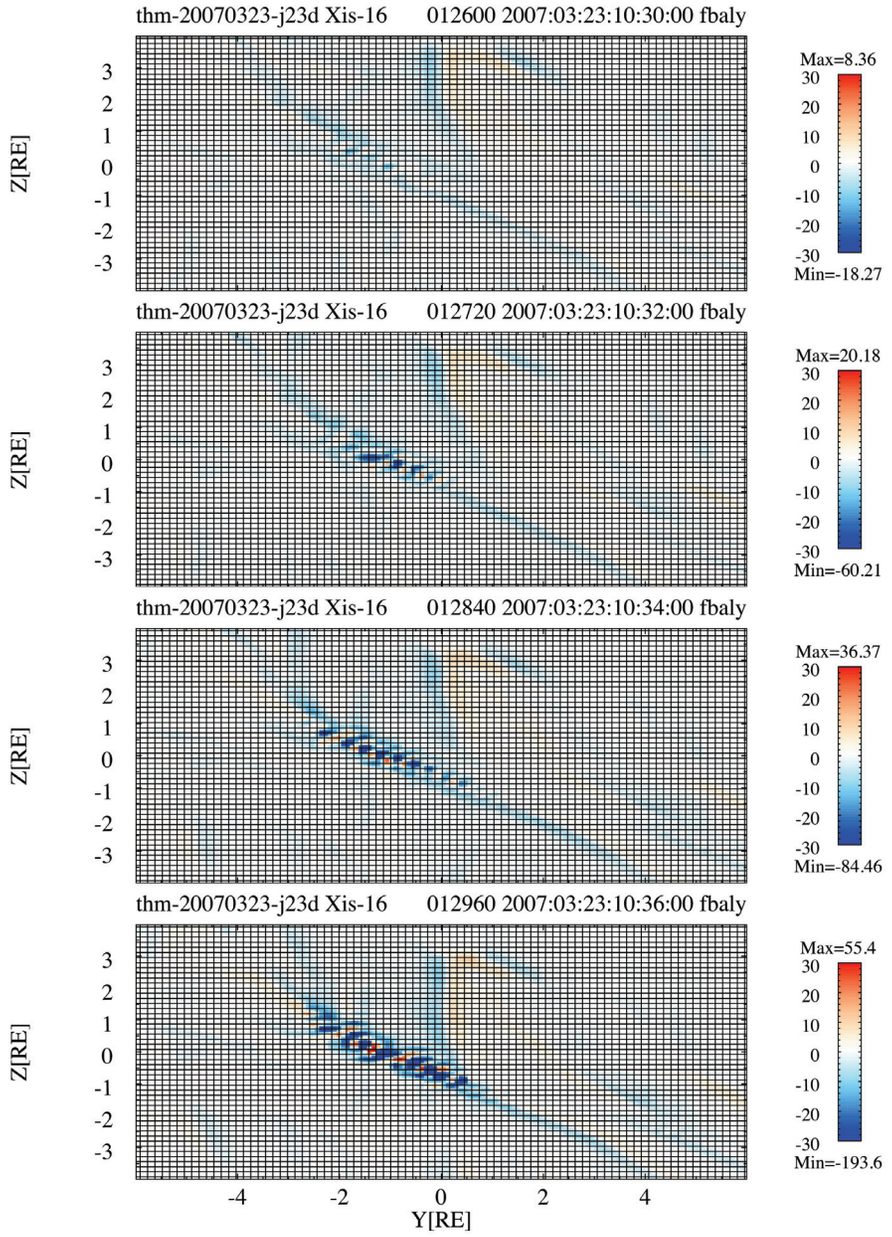

Figure 1. Cuts across the tail at $X_{GSE} = -16\ R_E$. The color coding shows the force imbalance in the y direction between the magnetic and the pressure forces in units of fN m^{-3}. The grid lines show the numerical grid used in the simulations. The ballooning waves are obviously sufficiently resolved.

We now wish to investigate possible auroral signatures of the ballooning growth in the tail. Auroral precipitation can be caused by several processes, in particular, by scattering of hot electrons into the loss cone and by the acceleration of electrons in auroral current sheets. The latter is associated with field-aligned currents (FACs) that originate in the magnetosphere. Other acceleration processes such as through kinetic Alfvén waves are also possible. The OpenGGCM does include the first two processes in a self-consistent manner. For example, *Raeder et al.* [2008] show the "discrete" (i.e., FAC-accelerated) precipitation for this event. However, we do not expect the ballooning mode structures to show up in the simulated precipitation. The structures are only marginally, but sufficiently, resolved in this simulation.

Grid lines are drawn in Figure 1 to show how the ballooning fingers compare to the grid. A full wave covers approximately five to seven cells, which is well beyond the grid Nyquist frequency. However, as the field lines from these structures converge toward the ionosphere, the waves are no longer resolved. Thus, for example, the FAC generated by a ballooning finger would dissipate numerically before reaching the inner boundary of the MHD domain (at 2.7 R_E) (see *Raeder* [2003] for a discussion of M-I mapping in the OpenGGCM.) In other words, field lines that are, for example, approximately five to seven cells apart in the tail will only be approximately one cell apart at the inner boundary of the MHD domain, and thus, they would no longer be numerically resolved.

In the real M-I system, however, no such restrictions apply. It may be any of the before-mentioned processes that direct electrons toward the ionosphere. Since we are primarily interested in the precipitation pattern, we may thus make the well-founded assumption that these processes would preserve the magnetic mapping, i.e., that the electrons would move faithfully along magnetic field lines from the generator region in the tail to the topside ionosphere. We thus proceed to map the tail structures magnetically to the ionosphere.

Figure 2 shows such a mapping. Here we choose again $\tilde{F}_y$ as the quantity to map, simply for the reason that the ballooning fingers show up best in $\tilde{F}_y$. We could have used almost any other fluid/field variable, such as the pressure or a field component. The only difference would be a less pronounced signature, but the geometry would be the same. For the mapping in Figure 2, we traced field lines from the ionosphere and colored the plot according to the value of $\tilde{F}_y$ at the tip of the field line, i.e., the part of the field line farthest from Earth. This technique allows to show the structure in its entire extent since a mapping from a specific distance might have shown only part of it. Comparison with Figure 5 of *Raeder et al.* [2010] shows that depending on distance and time, only part of the unstable structure would appear in such mapping.

The times in Figure 2 are chosen differently (earlier) than in Figure 1. It turns out that the mode is already growing *somewhere* along the mapping field lines before it shows up in the specific cut of Figure 1. Specifically, the times shown here are 10:20, 10:23, 10:26, and 10:30 UT, respectively, from top to bottom in the figure. Since the mapping only shows the closed field lines, one can see the open-closed boundary as the upper edge of the colored part. Note, however, that this boundary wraps upward away from the tail center. There is also a very distinct transition further equatorward that marks the inner edge of the plasma sheet. From this time sequence, it is clear that we are still in the late growth phase of the substorm as both boundaries keep drifting equatorward, and the polar cap still grows. The breakup occurs later. We will not analyze the breakup here any further, other than saying that it occurs *not* at the same location where the ballooning mode is present.

The morphology of the ionospheric signatures is very peculiar. First, the spacing of the "beads" (as they are often called in the literature) is approximately 2.2° in longitude, corresponding to an azimuthal wavenumber of $m \sim 160$. This compares very well to auroral images, both from the ground and from space, as shown by *Liang et al.* [2008] and by *Henderson* [2009]. That spacing is also consistent with a roughly radial mapping from the tail. Each wave crest is not simply a spot, but elongated in latitude, thus forming small streaks. These streaks all seem to be directed toward a point some 3°–4° to the north such that they seem to radiate from there. One should note, however, that these figures do not show luminosity, thus, the shape of these streaks in the real world may be different. Specifically, since the low-latitude part of each of the streaks maps closer to the Earth, and thus to hotter plasma, compared to the high-latitude parts, the visible structure may well look more like a dot. As time progresses, the streaks become more and more distorted, but also stronger, until they merge into a less well-defined structure. The similarities to the IMAGE FUV/WIC images of the 21 November 2002 substorm presented by *Henderson* [2009] are striking. In particular, the mode grows over several minutes prior to expansion phase onset and "disintegrates" ~2 min before the substorm expansion phase commences.

5. SUMMARY AND DISCUSSION

We presented results from an OpenGGCM simulation that show the development of the ballooning mode in the tail prior to expansion phase onset and how it maps into the ionosphere. We find our results to be consistent with observations in several respects, which lead to these findings:

1. The tail signatures, in particular the wavelength λ_y of the mode, are very close to observations, for example, those by *Saito et al.* [2008]. This is actually somewhat surprising because the OpenGGCM is an MHD model, while theoretical limits on λ_y are generally based on kinetic considerations.

2. Likewise, the ionosphere signatures are also in close accordance with observations. In particular, the azimuthal wavenumber matches what is typically observed. Furthermore, the timing and temporal development of the ionospheric "beads" closely matches one published observation of a substorm breakup.

3. Since the simulation produces both the tail and the ionosphere signatures and shows that they are linked, further evidence is provided that auroral "beads" are actually the counterpart of tail ballooning modes. Since the aurora is easier

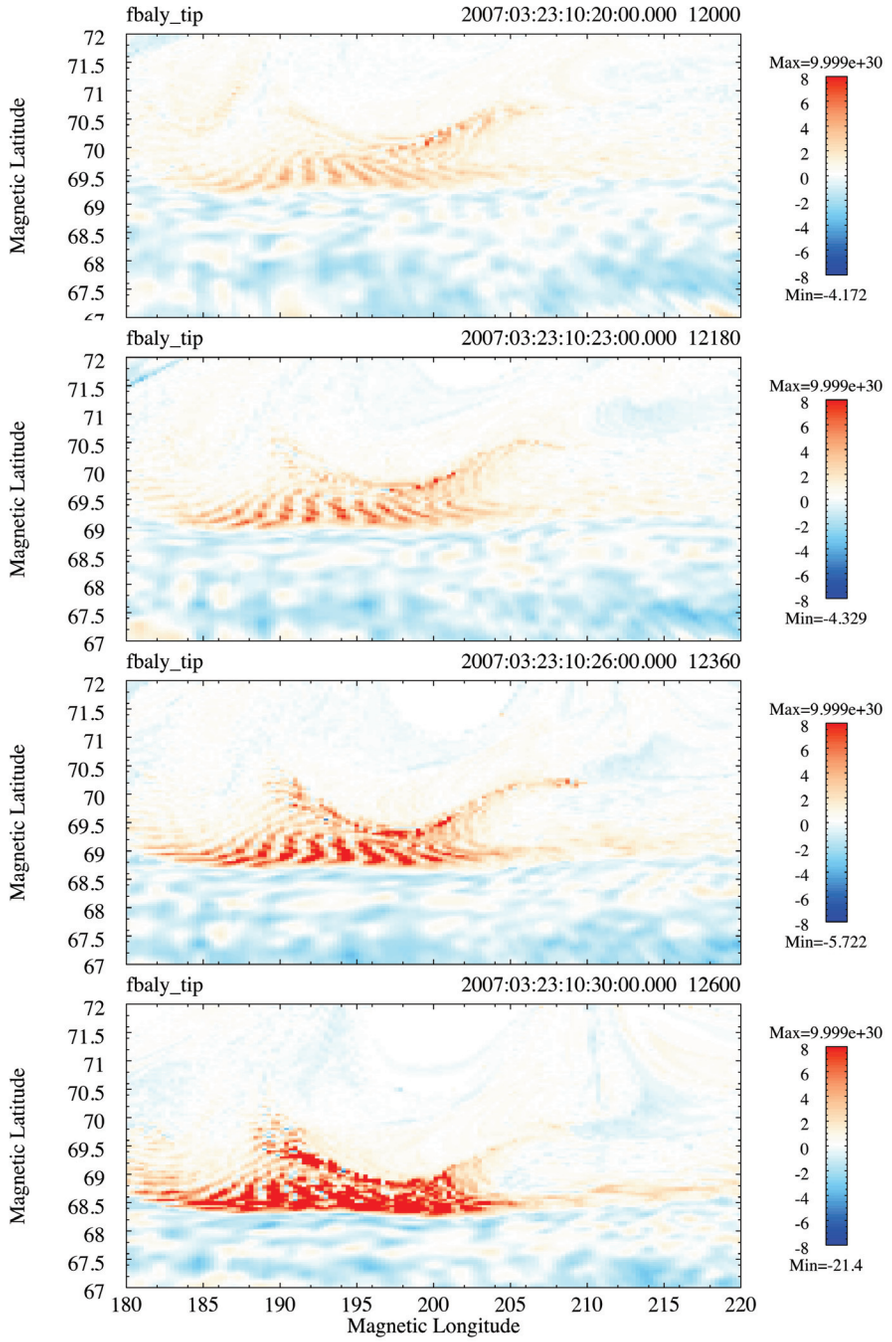

Figure 2. Ballooning modes mapped to the ionosphere. Field lines are traced from every location on the plot from the ionosphere through the magnetosphere. For field lines that are closed, the color coding is according to the same force imbalance shown in Figure 1 at the tip of the field line, in units of fN m^{-3}. The pattern seen is the expected pattern of ionospheric emissions caused by the ballooning mode. However, no statement about the luminosity can be made because we do not know the mechanism that would cause the aurora.

observed, in particular on a global level, than the tail, this will allow more extensive studies of the ballooning mode and its relation to substorm onset.

We note here that the ballooning mode occurs in the simulation not only prior to onset but also after onset. *Zhu et al.* [2009] has analyzed the stability condition using the OpenGGCM field and plasma parameters and found that the tail exceeds the marginal stability criterion at times and in regions where we find the ballooning signatures also.

In this paper, we purposely did not investigate the relation between the ballooning mode and expansion phase onset. As shown by *Raeder et al.* [2010], a second ideal-like mode (named the axial mode because it has zero azimuthal wavenumber) is present, which is more closely linked to tearing and may also be related to the so-called bubble-blob formation [*Hu et al.*, 2011]. This mode is now under investigation, and the results will be presented elsewhere. The mode is similar to the ballooning mode in the sense that it does not cause a magnetic topology change, but it also has features in common with the tearing mode, namely, that it requires some nonidealness of the plasma that allows at least for the partial decoupling of the flux tube motion from the flow. The relation between the ballooning mode and the axial mode is also still an open question. However, the simulation shows no evidence of the ballooning mode triggering tearing. If that were the case, one would expect tearing to start in the troughs of the ballooning mode where the B_z has a minimum. However, no such structuring of the tearing mode has been seen in the simulations.

Acknowledgments. This research was supported by NASA grant NAS5-02099 (THEMIS) and NSF grants ATM-0639658 and ATM-0902360. Development of the OpenGGCM has been supported by NASA grant NNG05GM57G and NSF grant ATM-0639658. G. L. S. was in part supported by NSF grant ATM-0809307. Part of the simulations was performed at the National Center for Supercomputer Applications (NCSA). Part of this work was accomplished while J. R. was on sabbatical at CESR, Toulouse, France. He would like to thank the CESR staff, and Benoit Lavraud in particular, for their hospitality and support.

REFERENCES

Angelopoulos, V., et al. (2008), First results from the THEMIS mission, *Space Sci. Rev.*, *141*, 453–476.

Bhattacharjee, A., Z. W. Ma, and X. Wang (1998), Dynamics of thin current sheets and their disruption by ballooning instabilities: A mechanism for magnetospheric substorms, *Phys. Plasmas*, *5*, 2001–2009, doi:10.1063/1.872871.

Cheng, C. Z., and S. Zaharia (2004), MHD ballooning instability in the plasma sheet, *Geophys. Res. Lett.*, *31*, L06809, doi:10.1029/2003GL018823.

Fuller-Rowell, T. J., D. Rees, S. Quegan, R. J. Moffett, M. V. Codrescu, and G. H. Millward (1996), A coupled thermosphere-ionosphere model (CTIM), in *STEP Report*, edited by R. W. Schunk, p. 217, Sci. Comm. on Sol. Terr. Phys. (SCOSTEP), NOAA/NGDC, Boulder, Colo.

Henderson, M. G. (2009), Observational evidence for an inside-out substorm onset scenario, *Ann. Geophys.*, *27*, 2129–2140.

Hu, B., F. R. Toffoletto, R. A. Wolf, S. Sazykin, J. Raeder, D. Larson, and A. Vapirev (2010), One-way coupled OpenGGCM/RCM simulation of the 23 March 2007 substorm event, *J. Geophys. Res.*, *115*, A12205, doi:10.1029/2010JA015360.

Hu, B., R. A. Wolf, F. R. Toffoletto, J. Yang, and J. Raeder (2011), Consequences of violation of frozen-in-flux: Evidence from OpenGGCM simulations, *J. Geophys. Res.*, *116*, A06223, doi:10.1029/2011JA016667.

Kepko, L., M. G. Kivelson, and K. Yumoto (2001), Flow bursts, braking, and Pi2 pulsations, *J. Geophys. Res.*, *106*, 1903–1915, doi:10.1029/2000JA000158.

Kepko, L., et al. (2008), Highly periodic stormtime activations observed by THEMIS prior to substorm onset, *Geophys. Res. Lett.*, *35*, L17S24, doi:10.1029/2008GL034235.

Lee, D.-Y., and K. W. Min (1996), On the possibility of the MHD-ballooning instability in the magnetotail-like field reversal, *J. Geophys. Res.*, *101*(A8), 17,347–17,354.

Lee, D.-Y., and R. A. Wolf (1992), Is the Earth's magnetotail balloon unstable?, *J. Geophys. Res.*, *97*(A12), 19,251–19,257.

Liang, J., E. F. Donovan, W. W. Liu, B. Jackel, M. Syrjäsuo, S. B. Mende, H. U. Frey, V. Angelopoulos, and M. Connors (2008), Intensification of preexisting auroral arc at substorm expansion phase onset: Wave-like disruption during the first tens of seconds, *Geophys. Res. Lett.*, *35*, L17S19, doi:10.1029/2008GL033666.

Liang, J., W. W. Liu, E. F. Donovan, and E. Spanswick (2009), In-situ observation of ULF wave activities associated with substorm expansion phase onset and current disruption, *Ann. Geophys.*, *27*, 2191–2204.

Miura, A. (2001), Ballooning instability as a mechanism of the near-Earth onset of substorms, *Space Sci. Rev.*, *95*, 387–398.

Ohtani, S.-I., and T. Tamao (1993), Does the ballooning instability trigger substorms in the near-Earth magnetotail?, *J. Geophys. Res.*, *98*(A11), 19,369–19,379.

Pu, Z. Y., A. Korth, Z. X. Chen, R. H. W. Friedel, Q. G. Zong, X. M. Wang, M. H. Hong, S. Y. Fu, Z. X. Liu, and T. I. Pulkkinen (1997), MHD drift ballooning instability near the inner edge of the near-Earth plasma sheet and its application to substorm onset, *J. Geophys. Res.*, *102*(A7), 14,397–14,406.

Pu, Z. Y., et al. (1999), Ballooning instability in the presence of a plasma flow: A synthesis of tail reconnection and current disruption models for the initiation of substorms, *J. Geophys. Res.*, *104*(A5), 10,235–10,248.

Raeder, J. (2003), Global magnetohydrodynamics – A tutorial, in *Space Plasma Simulation*, *Lect. Notes Phys.*, vol. 615, edited by J. Büchner, C. T. Dum, and M. Scholer, p. 212–246, Springer, Berlin.

Raeder, J., Y. Wang, and T. J. Fuller-Rowell (2001a), Geomagnetic storm simulation with a coupled magnetosphere-ionosphere-thermosphere model, in *Space Weather*, *Geophys. Monogr. Ser.*, vol. 125, edited by P. Song, H. J. Singer, and G. L. Siscoe, pp. 377–384, AGU, Washington, D. C., doi:10.1029/GM125p0377.

Raeder, J., R. L. McPherron, L. A. Frank, S. Kokubun, G. Lu, T. Mukai, W. R. Paterson, J. B. Sigwarth, H. J. Singer, and J. A. Slavin (2001b), Global simulation of the Geospace Environment Modeling substorm challenge event, *J. Geophys. Res.*, *106*, 381–395, doi:10.1029/2000JA000605.

Raeder, J., D. Larson, W. Li, E. L. Kepko, and T. Fuller-Rowell (2008), OpenGGCM simulations for the THEMIS mission, *Space Sci. Rev.*, *141*, 535–555, doi:10.1007/s11214-008-9421-5.

Raeder, J., P. Zhu, Y. Ge, and G. Siscoe (2010), Open Geospace General Circulation Model simulation of a substorm: Axial tail instability and ballooning mode preceding substorm onset, *J. Geophys. Res.*, *115*, A00I16, doi:10.1029/2010JA015876.

Runov, A., V. Angelopoulos, N. Ganushkina, R. Nakamura, J. McFadden, D. Larson, I. Dandouras, K.-H. Glassmeier, and C. Carr (2008), Multi-point observations of the inner boundary of the plasma sheet during geomagnetic disturbances, *Geophys. Res. Lett.*, *35*, L17S23, doi:10.1029/2008GL033982.

Saito, M. H., Y. Miyashita, M. Fujimoto, I. Shinohara, Y. Saito, K. Liou, and T. Mukai (2008), Ballooning mode waves prior to substorm-associated dipolarizations: Geotail observations, *Geophys. Res. Lett.*, *35*, L07103, doi:10.1029/2008GL033269.

Vetoulis, G., and L. Chen (1994), Global structures of Alfvén-ballooning modes in magnetospheric plasmas, *Geophys. Res. Lett.*, *21*(19), 2091–2094.

Zhu, P., A. Bhattacharjee, and Z. W. Ma (2004), Finite k_y ballooning instability in the near-Earth magnetotail, *J. Geophys. Res.*, *109*, A11211, doi:10.1029/2004JA010505.

Zhu, P., C. R. Sovinec, C. C. Hegna, A. Bhattacharjee, and K. Germaschewski (2007), Nonlinear ballooning instability in the near-Earth magnetotail: Growth, structure, and possible role in substorms, *J. Geophys. Res.*, *112*, A06222, doi:10.1029/2006JA011991.

Zhu, P., J. Raeder, K. Germaschewski, and C. C. Hegna (2009), Initiation of ballooning instability in the near-Earth plasma sheet prior to the 23 March 2007 THEMIS substorm expansion onset, *Ann. Geophys.*, *27*, 1129–1138.

Y. Ge and J. Raeder, Space Science Center and Physics Department, University of New Hampshire, 8 College Rd, Durham, NH 03824, USA. (Yasong.Ge@gmail.com, J.Raeder@unh.edu)

G. Siscoe, Center for Space Physics, Boston University, 725 Commonwealth Ave., Boston, MA 02215, USA. (siscoe@skynet.bu.edu)

P. Zhu, Department of Engineering Physics, University of Wisconsin-Madison, 1500 Engineering Dr., Madison, WI 53706, USA. (pzhu@wisc.edu)